Seismic Performance Analysis of Reinforced Concrete Frame Structures Based on Computational Mechanics

Taochun Yang[1,*], Yanjun Li[2] and Xiaohui Zhai[3]

[1]*College of Civil Engineering and Architecture, Zhejiang University, Hangzhou 310027, China*
[2]*School of Civil Engineering and Architecture, University of Jinan, Jinan 250022, China*
[3]*Ningbo Jiangong Engineering Group Co., Ltd., Ningbo 315040, China*
E-mail: cea_yangtc@ujn.edu.cn
[*]*Corresponding Author*

Received 21 May 2021; Accepted 08 June 2021;
Publication 20 July 2021

Abstract

In order to study the degradation law and seismic performance of reinforced concrete frame structure with the extension of service time under normal service environment, the multi-scale modeling of corroded reinforced concrete frame is carried out by using the general finite element analysis software ABAQUS. The correctness of the multi-scale modeling method is verified by the experimental data of corroded reinforced concrete members and single frame. The pushover analysis and elastic-plastic time history analysis of a four story reinforced concrete frame structure are carried out by using a multi-scale model. Then the seismic response and damage of RC frame structures with different service time are compared. The experimental results show that the established seismic performance model of reinforced concrete frame structure is more practical in practical application and can meet the research requirements.

Keywords: Reinforced concrete, seismic performance, building structure.

European Journal of Computational Mechanics, Vol. 30_1, 99–120.
doi: 10.13052/ejcm1779-7179.3014

1 Introduction

The construction industrialization is an important part of the vigorously carrying out Urbanization Construction in China. As the key point to realize this key part, the development of assembly concrete structure is a hot spot in the design of concrete structure [1]. The assembly structure which is invested in the actual project has already reflected many advantages of it compared with the ordinary reinforced concrete structure, that is, it can improve the automation level and improve the efficiency, accelerate the project progress, reduce the site construction, and construct the whole process of green environment protection; it can meet the requirements of the green development of the construction industry. There are many shortcomings in assembly structure, so the reliability and integrity of assembly joints are difficult to meet the stress requirements under repeated loads [2]. For this reason, foreign scholars put forward a new type of composite structure - steel cage concrete structure, and carried out experimental research on the mechanical properties of steel cage concrete short columns and joints [3]. At present, the research on steel cage structure system is rare in China, which only stays in the research stage of members, and there is no achievement in the research of steel cage concrete frame structure, but some scholars have studied other aspects, for example, Wan Shicheng and others have carried out the test on the negative moment area of steel-concrete composite continuous beam strengthened with prestressed CFRP [4]; Zheng Leqi et al. Studied the mechanical behavior of concrete-filled steel tubular composite columns under eccentric compression [5]. In order to better supplement the relevant blank, this paper will study the seismic performance of prefabricated steel cage concrete frame. In the service process of reinforced concrete structure, under the action of human or natural factors, with the increase of service time, it will gradually aging, damage or even destroy. With the increase of service time, the durability problems such as concrete performance degradation and reinforcement corrosion will lead to the decrease of seismic performance and increase of seismic vulnerability. For the structure whose initial design meets the requirements of the specification, the seismic safety of the structure will be greatly reduced when it suffers serious durability damage. In order to ensure the seismic safety of reinforced concrete structure in the whole life cycle, it is necessary to evaluate the seismic performance of reinforced concrete structure based on time-varying. Based on this, this paper uses the finite element analysis software ABAQUS to carry out multi-scale modeling of corroded reinforced concrete frame. Through the test data of corroded

reinforced concrete members and single frame, the correctness of multi-scale modeling method is verified. Then the pushover analysis and elastic-plastic time history analysis of four story reinforced concrete frame structure are carried out by using multi-scale model. Finally, the seismic response and damage of reinforced concrete frame structure with different service time are compared, In order to carry out the mechanical modeling and analysis of the seismic performance of reinforced concrete frame structure.

2 Mechanical Modeling of Seismic Performance of Reinforced Concrete Frame Structure

2.1 Characteristic Parameters of Reinforced Concrete Structures With Low Ductility

As a new type of structural component, reinforced concrete has been used in the environment and technology level is improving, and the scale of reinforced concrete is gradually improved, which has been deeply rooted in people's lives. Reinforced concrete structure has many advantages. It can improve the bearing capacity [6], improve the plasticity and seismic performance [7, 8]. In this paper, reinforced concrete structure without seismic fortification or insufficient consideration of seismic design is defined as "low ductility structure" [9]. Taking such structure as the main research object, the improved numerical simulation method and seismic performance analysis are carried out according to the typical design characteristics of different types of members. On this basis, the characteristics of the low ductility reinforced concrete structure are analyzed.

From the perspective of structural design and construction: combined with the above literature review at home and abroad, the common design features of reinforced concrete low ductility structure are summarized, which are mainly divided into four aspects: insufficient restraint, insufficient anchorage, insufficient strength and sudden change of stiffness [10]. These design characteristics that affect the ductility of the structure can be reflected through its basic components, and may cause six types of failure i–vi. If the horizontal and vertical stiffness of the structure is discontinuous and irregular, it will lead to significant torsion effect or structural problems such as the first floor weakness [11]. It is more prominent in low ductility structure. From the perspective of the development of structural seismic codes, the possible failure types of reinforced concrete structures with low ductility are analyzed, which are not considered in seismic fortification or seismic design.

Table 1 Characteristics of reinforced concrete structures with low ductility

Low Ductility Characteristics/Member Types		Template	Shear Wall	Node	Column	Beam	Possible Failure Types
Insufficient anchorage	Stirrup without hook or irregular 90° hook		√	√	√	√	Type I,II
	The anchorage length of longitudinal reinforcement is not enough		√		√		Type III
	The bending zone of longitudinal reinforcement is cut off too early					√	Type V
Insufficient constraints	No stirrup			√			Type I,II
	Stirrup configuration is simple				√		Type I,II
	Stirrup spacing is large and diameter is small		√	√	√	√	Type I,II
Insufficient strength	The performance of concrete material is poor	√	√	√	√	√	/
	The ratio of longitudinal reinforcement is low		√		√	√	/
	The overlapping position of longitudinal bars is unfavorable		√		√		Type III
Stiffness burst	Vertical discontinuity of lateral force resisting member		√		√		/
	Vertical irregularity of lateral force resisting members		√		√		/
	Irregular structure plane design						/

Table 2 Possible failure types of reinforced concrete structures with low ductility

	Possible Failure Types	Explain
Type I	Longitudinal bar lap failure	The lap failure is caused by insufficient lap length of longitudinal bars, insufficient lateral restraint and complex stress at lap position
Type II	Bond failure of reinforcement	It mainly refers to plain round reinforcement, including anchorage failure caused by bond failure
Type III	Reinforcement anchorage failure	Failure due to too short anchorage length or in complex zone
Type IV	Buckling of longitudinal bars under compression	The lateral buckling of stirrups is insufficient due to the excessive spacing of stirrups
Type V	Impact shear failure	Failure mode of slab column connection caused by discontinuous reinforcement
Type VI	Shear brittle failure	Columns, beam column joints, shear walls and other components may occur

Reinforced concrete structure is the most widely used structural form for human beings. A large number of numerical models and simulation methods have been carried out for this kind of structure, and the number of related achievements and literatures is huge [12]. According to the practical experience and literature review, the common numerical models of reinforced concrete beams, columns, joints, shear walls, floors and other basic components are divided into five categories according to the geometric properties and stress characteristics of various models, which are based on point element (hinge), line element, surface element, volume element, and the combined element formed by the combination of the above four types of elements At present, quasi-static test and shaking table test are the main means to study reinforced concrete low ductility structure and its components, while the research with refined finite element numerical simulation is relatively less and less systematic [13]. Considering that the mechanical performance of the key components prone to brittle failure may directly affect the ultimate failure mode of the structure, but a large number of existing numerical models and simulation methods are developed for ductile structures and components, and most of them fail or are not easy to consider the influence of brittle failure of these key components on the overall seismic performance and failure mode of the structure [14]. Combined with OPENSEES (Open System for Earthquake

Engineering Simulation), an open source software for seismic engineering simulation, this paper briefly introduces the numerical models and simulation methods of each component based on point element, line element, surface element and volume element. On this basis, it focuses on the detailed numerical simulation methods of low ductility structures and components formed by the combination of the above four types of elements [15]. The seismic vulnerability function can be divided into two types, namely, the vulnerability function based on ground motion intensity and the vulnerability function based on displacement.

$$F_{R,\mathrm{IM}}(x) = \Phi\left[\frac{\ln\left(x/m_R\right)}{\beta_R}\right] - \mathrm{n} \tag{1}$$

Where: Φ is the standard normal cumulative distribution function, and m_R and β_R are the median value and logarithmic standard deviation of the seismic vulnerability function. *FR*, *IM*(*x*) are taken as the probability distribution of the generalized seismic capacity R of the structure expressed by the seismic intensity [16]. The median vulnerability value m_R can be regarded as the representative value of the generalized seismic capacity R of the structure, which represents the average seismic capacity level of the structure corresponding to different limit states. When evaluating the seismic collapse resistance of structures, fema-p695 puts forward the concept of "collapse margin ratio", that is, the ratio of the median collapse capacity of structures to the intensity of rare earthquakes, to measure the seismic collapse safety margin of structures [17]. Based on the concept of CMR, the seismic performance margin corresponding to different limit states under the action of frequent earthquake, fortification earthquake and rare earthquake is comprehensively evaluated.

$$\alpha_{\mathrm{FE}} = F_{R,\mathrm{IM}}(x) - \frac{m_R}{S_{a,\mathrm{FE}}} \tag{2}$$

$$\alpha_{\mathrm{DBE}} = F_{R,\mathrm{IM}}(x) + \frac{m_R}{S_{a,\mathrm{DBE}}} \tag{3}$$

$$\alpha_{\mathrm{RE}} = \frac{m_R}{S_{a,\mathrm{RE}}} - F_{R,\mathrm{IM}}(x) \tag{4}$$

Where: S_a, $F_{R,\mathrm{IM}}$, S_a, DBE are the acceleration of seismic dynamic spectrum corresponding to frequent earthquake, fortification earthquake and rare earthquake respectively; α_{FE}, α_{DBE} and α_{RE} represent the performance margin ratio of structure under frequent earthquake, fortification earthquake

and rare earthquake respectively

$$F_{R,D}(x) = \alpha_{\mathrm{FE}} - \alpha_{\mathrm{DBE}} - \alpha_{\mathrm{RE}}/\Phi\left[\frac{\ln m_{DIS_a} - \ln m_C}{\sqrt{\beta_{DIS_a}^2 + \beta_C^2}}\right] \tag{5}$$

Where m_C is the median value of seismic capacity C of the structure corresponding to different limit states, the median value of seismic demand D for the structure under the action of S_a strength; β_C is the logarithmic standard deviation of seismic capacity and seismic demand. The basic assumption of seismic vulnerability function based on displacement is that under the action of seismic intensity S_a, the seismic demand D obeys the logarithmic normal distribution, and the seismic capacity C of the structure obeys the logarithmic normal distribution. Among them, the probability seismic demand parameters. Generally, the "cloud chart" method can be used to obtain the parameters of probability earthquake demand by logarithmic linear regression of the nonlinear time history analysis results of the structure.

$$\ln m_{DIS_a} = a_0 + a_1 \ln S_a F_{R,D}(x) \tag{6}$$

$$\beta_{DKS} = \sqrt{\frac{\sum_{i=1}^{N_{\mathrm{sm}}} \left[\ln D_i - \ln\left(m_{D1S}\right)\right]^2}{N_{\mathrm{RTR}} - 2}} \tag{7}$$

Where: a_0 and a_1 are regression parameters, and N is the number of seismic records to consider the variability of seismic records to the records; D_i represents the seismic demand under the action of ground motion in article i. According to the research results in the literature, the above hypothesis can better reflect the probability relationship between seismic demand and seismic intensity [18]. The vulnerability function based on displacement can be transformed into the vulnerability function based on the ground motion strength. The transformation process is

$$\begin{aligned} F_{R,D}(x) &= \Phi\beta_{DKS}\left(\frac{a_0 + a_1 \ln x - \ln m_C}{\sqrt{\beta_{D1S_e}^2 + \beta_C^2}}\right) \\ &= \Phi\beta_{DKS}\left(\frac{\ln x + \frac{a_0 - \ln m_C}{a_1}}{\frac{\sqrt{\beta_{DIS_a}^2 + \beta_C^2}}{\beta_1}}\right) \\ &= \Phi\beta_{DKS}\left(\frac{\ln\left(x/m'_R\right)}{\beta'_R}\right) \end{aligned} \tag{8}$$

Where: *m* and β are the median value and logarithmic standard deviation of the transformed seismic vulnerability function, respectively:

$$m'_R = F_{R,D}(x) \exp\left(\frac{\ln m_C - a_0}{a_1}\right) = \left(\frac{m_C}{\exp a_0}\right)^{1/a_1} \tag{9}$$

$$\beta'_R = \frac{\sqrt{\beta^2_{D1S_\alpha} + \beta^2_C}}{m'_R - a_1} \tag{10}$$

The above formula reflects the consistency of the vulnerability function based on the ground motion intensity and the vulnerability function based on the displacement. Most of the numerical models are based on zero length elements, such as bending hinge, shear hinge, axial hinge and sliding hinge [19]. The point element and line element are combined to form a "beam hinge combination element". Then the nonlinear constitutive relationship of each type of plastic hinge is determined by experimental means or empirical formula to consider the nonlinear response and brittle failure behavior of low ductility columns.

2.2 Special Shaped Mechanical Structure of Reinforced Concrete

The compressive and shear capacity of reinforced concrete is much higher than that of reinforced concrete. Compared with the steel column, although the compressive bearing capacity is slightly inferior, the local instability does not appear. Because the plasticity of reinforced concrete is improved, the brittle failure of concrete is prevented, and the axial compression ratio is no longer limited in high-rise buildings. At the same time, the cross-sectional area can be reduced by more than 50% compared with ordinary concrete members. Moreover, reinforced concrete can also participate in the advantages of large column network and large space in the frame system, which increases the use area by about 5% compared with reinforced concrete structure. As the cross-section becomes smaller, the self weight of reinforced concrete decreases greatly, and the seismic response also decreases accordingly. According to the relevant research and analysis, reinforced concrete columns and other structural systems used in high-rise buildings can reduce the self weight of reinforced concrete structure by one-third to one-half, and reduce the seismic effect by half. At the same time, by reducing the column section, the unit area load on the foundation can be reduced by more than 25%, the corresponding foundation size is also reduced, and the project cost

is reduced. In addition, the concrete filled in the steel tube can consume a lot of heat in case of fire, the temperature field of the column section is uneven, and the fire resistance time of the column is extended [20, 21]. Among them, the point line combination element is formed by beam and hinge element, the more typical one includes equivalent frame element and multi vertical bar element, while the line line combination element is mainly formed by different line elements, the more typical one is the frame analysis model composed of bar element and bar element, the beam bar model composed of beam element and bar element, and the similar frame model composed of beam element and beam element In this paper, the element composed by the similar method is called "bar system combined element". The wall is simplified as equivalent column, which is placed at the central axis of the wall. The rigid bar is set at each floor to connect with the floor beam element, and the zero length element is set at the joint of the rigid bar with the equivalent column and beam element, which can be used to simulate the nonlinear behavior of steel bar slip, bending deformation and so on. The modeling method of the element is simple and the calculation efficiency is high, but the movement of the neutral axis of the cross section of the shear wall is not considered, and the horizontal shear deformation of the shear wall cannot be considered. A three vertical bar element is proposed. Three vertical bar elements, horizontal shear spring and rotating spring are used to simulate the bending and shear deformation behavior of shear wall members. Multiple spring elements are used to simulate the axial, bending and shear mechanical performance of the whole wall. A multi vertical bar element is proposed.

The appearance of special-shaped reinforced concrete column combines reinforced concrete column and special-shaped reinforced concrete column. Steel tube and core concrete resist axial force together, and steel tube has restraint effect on core concrete. Compared with reinforced concrete, it not only improves the bearing capacity, stiffness, plasticity and seismic performance, but also has the advantages of good impact resistance and fatigue resistance. Moreover, the thickness of the column is the same as that of the infilled wall, which makes the interior corners flat, increases the indoor space and makes the home layout free. In addition, special-shaped reinforced concrete columns can make up for the shortcomings of high stirrup ratio and low limit value of axial compression ratio of special-shaped reinforced concrete columns, and make high-strength concrete participate in the building structure. In the nonlinear analysis of structure, the nonlinear constitutive relation of material should be determined by experiment, and the verified mathematical model can also be used. Short leg shear wall is a kind of

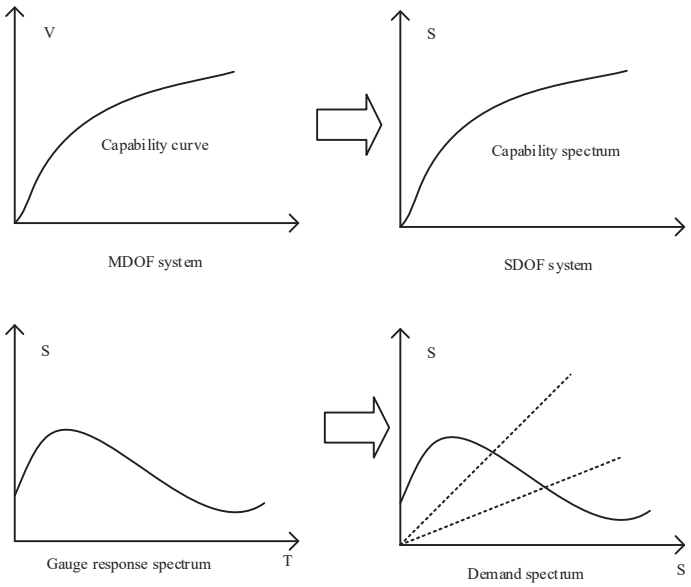

Figure 1 Capacity spectrum, demand spectrum and performance change of reinforced concrete structure.

component form between special-shaped column and shear wall. Its mechanical properties and failure mechanism are different from both special-shaped column and general shear wall. On the basis of previous research, the strength and ductility of short leg shear wall are investigated, and the changes of strength and ductility when the height thickness ratio and axial compression ratio of the wall are changed.

Table 3 Mechanical indexes of materials

Concrete	A Steel Bar
Axial compressive strength f_c 24.5	Yield strength f_y 361.59
Modulus of elasticity E_C 3.18×10^4	Modulus of elasticity E_4 2.1×10^5

When the load of the member reaches the maximum, the load decreases with the increase of the deformation, and then the section completely loses the bearing capacity. In the design of the bearing capacity of members, it refers to the maximum value of the initial load. In the calculation of materials by software, it is usually simplified according to the characteristics of various materials. In the calculation of steel, a special material, the software will

merge its constitutive relationship approximately from a curve and simplify it to straight lines at both ends, which is the double broken line model. The software provides users with two types of double broken line model, which is the same as the above theory. One is the double broken line model with follow-up strengthening characteristics, which is the most commonly used model form; the other is the double broken line model with isotropic strengthening function. The yield criteria used in the two models are the same, and von Mises stress-strain curves are used in both models. For the definition of steel in this simulation, the double broken line follow-up strengthening model is used to simulate, because the final diagram includes the load displacement curve, which contains a special characteristic of steel and other metal materials, Bauschinger effect; This effect is due to the metal material in the process of forward loading into the plastic deformation, which makes the material soften under reverse loading and weaken the yield property of the material.

When the flange is under compression, the bending capacity of the T-shaped short leg shear wall is 209.81 kn/m; when the horizontal load is reversed, that is, when the flange is under tension, the bending capacity of the T-shaped short leg shear wall is 168.05 kn/m. From the situation of flange tension, the ductility of T-section short leg shear wall is very low, but the seismic analysis results of the whole structure show that when the short leg shear wall structure is symmetrically arranged, when the horizontal load is reversed, some short leg shear wall flanges are located in the compression area, and the axial compression ratio limits of special-shaped column and short leg shear wall are given according to the seismic grade. According to the seismic grade of high-rise building structure with A-level height specified in the high-rise building code, the seismic grade of special-shaped column frame structure and short leg shear wall structure is shown in the table.

Table 4 Seismic grade of special-shaped column frame structure and short limb scissor wall structure

Structure Type		Earthquake Intensity		
		8 Degrees	7 Degrees	6 Degrees
Short leg shear wall structure	Height(m)	$\leq$80	$\leq$80	$\leq$80
	Short leg shear wall	one	two	three
Special shaped column frame	Height(m)	$\leq$30	$\leq$30	$\leq$30
	frame	two	three	four

The frame structure with special-shaped columns is generally only used in multi-storey buildings, so the seismic grade of frame structure with height less than 30 m is only given in the table. As the short leg shear wall structure is shorter than the general shear wall structure, its seismic performance is worse. It is suggested that it should only be used in small high-rise buildings with 8–15 floors, so only the seismic grade of short leg shear wall structure with height less than 80 m is given. According to the provisions of seismic grade of special-shaped column frame structure and short leg shear wall structure, and according to the values of axial compression ratio limits of special-shaped column and short leg shear wall in the table, the axial compression ratio limits of members in special-shaped column frame structure and short leg shear wall structure are summarized as follows.

Table 5 Limit values of axial compression ratio for special shaped columns and short leg shear walls

	Earthquake Intensity		
Structure Type	8 Degrees	7 Degrees	6 Degrees
Short leg shear wall	0.5	0.6	0.7
Special shaped column frame	0.5	0.6	0.7

The limit value of axial compression ratio of short leg shear wall in the table does not include the *I*-shaped short leg shear wall without flange or end column. The limit value of axial compression ratio of special-shaped columns is the minimum value of axial compression ratio of *T*-shaped, *L*-shaped and cross-shaped columns, and the limit value of axial compression ratio of short leg shear wall is given in the code. It can be seen from the table that the limit value of axial compression ratio of special-shaped column and short leg shear wall can be consistent, which indicates that there is no clear boundary between the mechanical characteristics of special-shaped column and short leg shear wall, and it is sometimes inconvenient to quantitatively distinguish the boundary between them.

2.3 Realization of Aseismic Design of Reinforced Concrete Structure

To establish a reasonable nonlinear finite element analysis model is the key to analyze the mechanical properties of reinforced concrete structure, especially to establish a reasonable model to analyze the complex structure of reinforced concrete composite special-shaped columns. In this paper, the large-scale

finite element simulation software ABAQUS is used to establish the joint model of reinforced concrete composite L-shaped special-shaped column, and the calculation is carried out to study the seismic performance of special-shaped column under different axial compression ratio, so as to provide the basis for the design and calculation. This is because ABAQUS has a strong advantage of nonlinear analysis, which can do the mechanical and multi physical field analysis of a single part. At the same time, it can also do system level analysis and research. In order to improve the accuracy of simulation analysis, this paper uses ABAQUS for related research.This chapter mainly describes the key problems in the process of modeling L-shaped column using ABAQUS, including the selection of steel and concrete constitutive, the setting of contact surface, the setting of loading mode, constraint mode and analysis step. When the steel is in different stress state, the structural relationship is naturally different. When the material is under monotonic and cyclic loading, the stress-strain relationship is different. Under the same monotonic load, the relationship curve can be divided into linear, bilinear and trilinear models. Isotropic properties are applied to the steel in the software. When the material is in the non-linear stage due to the force, the von Mises model of follow-up strengthening is used for steel. The stress-strain curve of steel is modeled by bilinear model

$$\sigma_e = \frac{1}{\sqrt{2}}\sqrt{(\sigma_1 - \sigma_2)^2 + (\sigma_2 - \sigma_3)^2 + (\sigma_3 - \sigma_1)^2} \tag{11}$$

Considering the hardening of steel bar and steel plate, this paper selects the reference constitutive relation model. The steel pipe, steel plate and steel bar are made of bilinear elastic-plastic material. The stress-strain curve is shown in the figure, which mainly reflects the stress-strain changes of the structure in the yield stage and ultimate stage. The hardening of the material in the plastic stage is mainly included in this model. HRB400 grade steel bar, HRB335 grade stirrup, Q235 steel pipe and batten plate are used in the structure. The same elastic modulus $E = 200$ GPa, Poisson's ratio $y = 0.3$, yield strain 0.0016 and ultimate strain 0.025 are adopted for steel pipe, steel plate and steel bar.

The plastic damage model of concrete combines isotropy, elastic damage and plastic tension and compression to simulate the nonlinear behavior of materials. It is assumed that the concrete has two failure mechanisms of tensile cracking and crushing failure. The evolution of yield surface and failure surface is managed by variables. The stress-strain curve of concrete

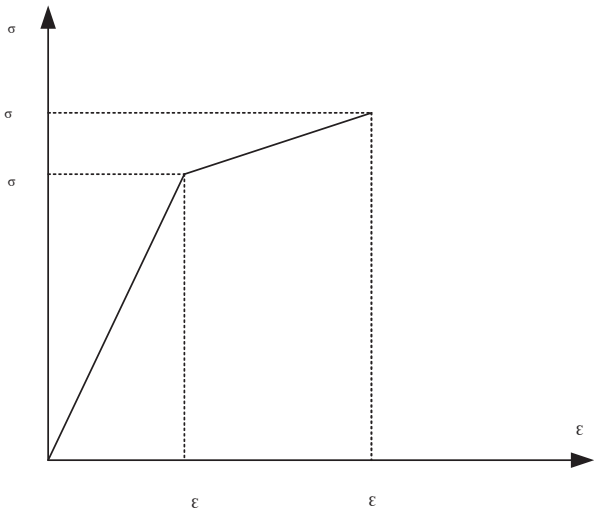

Figure 2 Stress strain curve of reinforced concrete.

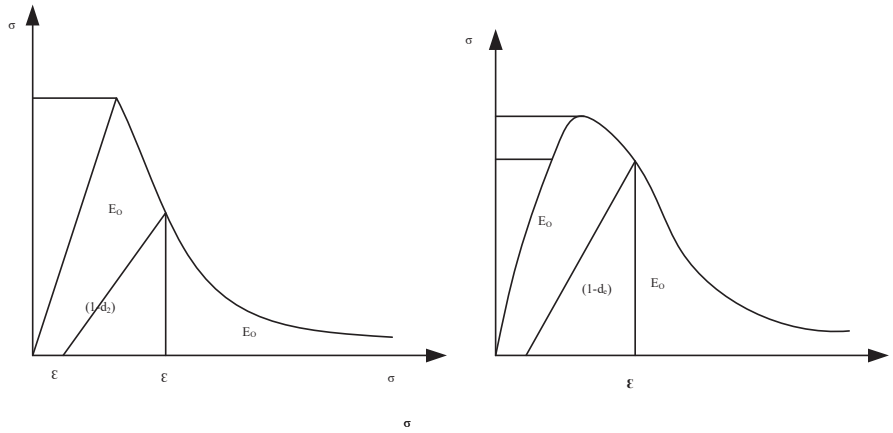

Figure 3 Constitutive relation curves of concrete damage plastic model under uniaxial tension and compression.

considering plastic damage is shown in the figure. The tensile cracking strain and compressive peak strain of concrete are 0.002.

When the concrete is under uniaxial compression, the stress-strain curve is linear in the initial stage. When the stress reaches the yield strength under pressure, the stress-strain curve becomes nonlinear. When the concrete reaches the maximum value of ultimate compressive strength, the concrete

softens under compression and the equivalent plastic strain of compression is:

$$\tilde{\varepsilon}_c^{pl} = \tilde{\varepsilon}_t^{in} - \frac{d_c}{1-d_c}\frac{\sigma_c}{E_c} \tag{12}$$

The stress of concrete considering compression damage is.

$$\sigma_c = (1-d_c)E_0\varepsilon_c^d = (1-d_c)E_0(\varepsilon_c - \varepsilon_c^{pl}) \tag{13}$$

The effective compression stress is.

$$\bar{\sigma}_c = \frac{\sigma_c}{1-d_c} = E_0(\varepsilon_c - \varepsilon_c^{pl}) \tag{14}$$

The stress and strain in the initial stage of uniaxial tension of concrete is also assumed to be linear, until the stress reaches a higher value. After the cracking stress, the concrete will be softened under tension. It is assumed that the concrete will be unloaded when the stress is t, and the equivalent tensile plastic strain of concrete is:

$$\tilde{\varepsilon}_t^{pl} = \tilde{\varepsilon}_t^{d\dot{\alpha}} - \frac{d_t}{1-d_t}\frac{\sigma_t}{E_0} \tag{15}$$

In the process of using ABAQUS finite element software to simulate, simplifying the boundary conditions of the model is an important program of finite element simulation analysis. The basic requirement of finite element simulation analysis is to make the finite element model consistent with the actual component as much as possible when the calculation can converge. However, it is difficult for us to establish the same model for some complex problems existing in the actual project, or the existing calculation program can not reach the height of simulating the actual situation. At this time, we need to appropriately simplify some secondary factors in the actual problems and establish a convenient model to reflect the actual research needs. In order to better distinguish the scope and avoid irrelevant analysis, the hinge constraint is applied to the lower end of the column, the chain constraint is applied to the side of the beam, and the boundary condition is applied to all the analysis steps.

3 Analysis of Experimental Results

According to the experimental results and theoretical analysis, T-shaped, L-shaped, cross shaped, Z-shaped special-shaped columns and short leg shear

wall members often have the characteristics of biaxial eccentric compression when they are stressed in the axial direction of the project. The compression and tension of special-shaped column and short leg shear wall flange are two typical cases, and their performance is representative. Therefore, following the research method of symmetrical section column, it is analyzed according to the one-way eccentric compression member. Because the experimental models of special-shaped columns and short leg shear wall structures are composed of T-shaped columns, the next analysis of the strength and ductility of special-shaped columns and short leg shear wall components mainly focuses on T-shaped section. Previous studies mainly focused on the strength and ductility analysis of experimental members, using the whole process analysis program and the comparative analysis of compression bearing capacity calculation formula of members, focusing on the influence of axial compression ratio, longitudinal reinforcement ratio, section size and other factors on the strength and ductility performance of special-shaped columns and short leg shear wall members, trying to understand the characteristics of such members more comprehensively. The section size and reinforcement of the T-shaped column used in the test of the research group are shown in the figure, and the measured values of the material mechanical properties are used, as shown in the table.

Table 6 Properties of materials (unit: N/mm^2)

Concrete	A Steel Bar
Axial compressive strength f_c 24.5	Yield strength f_y 305.16
Modulus of elasticity E_C 3.18×10^4	Modulus of elasticity E_4 2.1×10^5

The seismic vulnerability curve of the structure is obtained by combining the probabilistic seismic demand parameter and the probabilistic seismic capacity parameter, as shown in the figure.

Table 7 Probabilistic seismic capacity parameters

Capability Parameters	Total Destruction	Serious Damage	Moderate Damage	Slight Damage
βc	0.3	0.3	0.3	0.3
$m_c\|\theta_{max}$	4%	2%	1%	1/550

Based on the above data, the change of seismic vulnerability curve of reinforced concrete structure is further analyzed.

Table 8 Vulnerability function parameters based on seismic intensity

Model Number	Vulnerability Parameters	Total Destruction	Serious Damage	Moderate Damage	Slight Damage
F-5-1	β_R	0.63	0.65	0.56	0.63
	m_R	0.06g	0.31g	0.63g	1.39g
F-5-2	β_R	0.48	0.54	0.58	0.50
	m_R	0.07g	0.39g	0.84g	1.89g
F-5-3	β_R	0.45	0.53	0.63	0.63
	m_R	0.08g	0.56g	1.31g	2.96g
F-5-4	β_R	0.41	0.49	0.48	0.58
	m_R	0.09g	0.64g	1.47g	3.24g

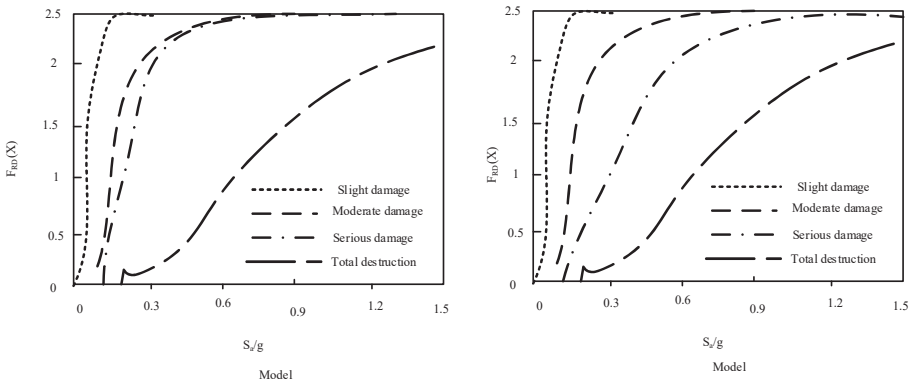

Figure 4 Seismic vulnerability curve of reinforced concrete structure.

In order to study the influence of section size on the limit value of axial compression ratio of special-shaped columns, the standard value of limit value of axial compression ratio of three typical sections of 200 × 600 × 200 × 600 × 700 × 200 × 700 and 200 × 800 × 200 × 800 T-shaped columns is calculated by using the whole process analysis program. In the calculation, the longitudinal reinforcement ratio is 1.2%, the end reinforcement of T-shaped column web is 0.7 times that of flange reinforcement, and the end reinforcement of TL shaped column is also 0.7 times that of column limb reinforcement perpendicular to it. Through the previous research, it is found that for each load angle, when the web is compressed, the standard value of

axial compression ratio of T-shaped and L-shaped column is the lowest. The calculation results are shown in the table.

Table 9 Limit values of axial compression ratio of special-shaped columns with different column height thickness ratio

Column Height Thickness Ratio	4	3.5	3
L-shaped column	0.45	0.38	0.20
T-shaped column	0.16	0.18	0.22

As shown in the table. In order to analyze the influence of structural fortification level on the parameters of seismic vulnerability function, the median value and logarithmic standard deviation of seismic vulnerability function corresponding to different structures are compared respectively. The bending moment curvature curves of flange compression and flange tension are obtained by FORTRAN program when the axial compression ratio is 0.1 and 0.5 respectively, as shown in the figure.

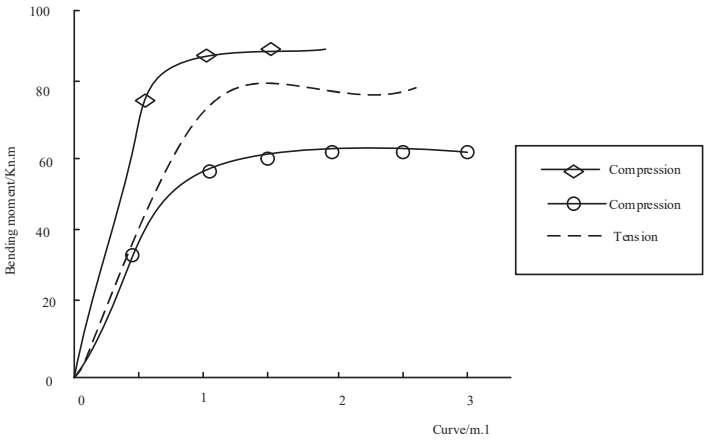

Figure 5 Relation curve of reinforced concrete under compression or tension.

It can be seen from the figure that with the improvement of the structural fortification level, the generalized seismic capacity r of the structure has been effectively improved, and the median value of the seismic vulnerability function also increases. It can be seen from the figure that with the improvement of the seismic fortification level of the structure, the logarithmic standard deviation of the seismic vulnerability function has decreased to a certain extent. The main reason is: for the structure with the same plane

layout and the same height, while improving the fortification intensity, the stiffness of the structure is increased, so as to reduce the deformation of the structure under the action of earthquake, so as to weaken the variability of seismic vulnerability to a certain extent. The seismic behavior of L-shaped reinforced concrete composite special-shaped columns with different axial compression ratio is studied, which provides theoretical reference for design and calculation. By using ABAQUS finite element software, the failure of L-shaped reinforced concrete composite special-shaped column joints under monotonic horizontal load and low cycle reciprocating load is simulated under axial compression ratio of 0, 0.2, 0.4, 0.5, 0.6, 0.7, 0.8, 0.9, 1.0, and the stress changes of column joints with different horizontal displacement directions are investigated. Through ABAQUS finite element simulation, the load displacement hysteretic curve from loading to failure is obtained, so as to analyze the influence of different axial compression ratio on the seismic performance of L-shaped reinforced concrete column joints, such as bearing capacity, ductility and skeleton curve. Based on this research, the feasibility of theoretical basis for future research work is put forward, which is convenient for future experiments and research.

4 Conclusions

Based on the general finite element software ABAQUS, the finite element model of reinforced concrete shear wall with concealed columns is established, and the bearing capacity and stiffness degradation of the shear wall are analyzed. By comparing with the test results, the following conclusions can be obtained. Two element B31 and layered shell element can be used to simulate the lateral bearing capacity and stiffness degradation of composite shear wall. Compared with the experimental results, the effectiveness of the modeling method is verified, which can provide a reference for further seismic analysis of this kind of structural system. However, due to the time limit, no more methods have been tried to analyze it. Therefore, more methods need to be tried to improve the effectiveness of the modeling method and provide reference for the seismic analysis of this kind of structural system.

References

[1] Ibrahim E M, Abbas Z K . Effect of magnetic water on strength properties of concrete[J]. IOP Conference Series: Materials Science and Engineering, 2021, 1067(1):012002 (12 pp).

[2] Elzahra I H A, Al-Sherrawi M H . Enhancement of self-healing to mechanical properties of concrete[J]. IOP Conference Series Materials Science and Engineering, 2021, 1117(1):012026.
[3] Yang H, Jiao S, Sun P . Bayesian-Convolutional Neural Network Model Transfer Learning for Image Detection of Concrete Water-Binder Ratio[J]. IEEE Access, 2020, PP(99):1–1.
[4] Wan S, Huang Q, Guan J . Test on flexural behavior of steel-concrete composite beams strengthened with prestressed carbon fiber-reinforced polymer plates[J]. Harbin Gongye Daxue Xuebao/Journal of Harbin Institute of Technology, 2019, 51(3):80–87.
[5] Pouraminian M, Pourbakhshian S . Multi-criteria shape optimization of open-spandrel concrete arch bridges: Pareto front development and decision-making[J]. Military Operations Research, 2019, 16(5): 670–680.
[6] Zheng L Q, Li G H, Zhou J Z, et al. Behavior of three-chord concrete-filled steel tube built-up columns subjected to eccentric compression[J]. Journal of Constructional Steel Research, 2020, 177(482):106435.
[7] Lu Y, Zhang Q, Xue Y, et al. Hypervelocity penetration of concrete targets with long-rod steel projectiles: experimental and theoretical analysis[J]. International Journal of Impact Engineering, 2021, 148(2):103742.
[8] Zhang X, Yang Z J, Huang Y J, et al. Micro CT Image-based Simulations of Concrete under High Strain Rate Impact using a Continuum-Discrete Coupled Model[J]. International Journal of Impact Engineering, 2021, 149(10):103775.
[9] Evstratova A V, Krishtalevich A K, Belov V V, et al. Design of prefabricated reinforced concrete structures: comparative analysis of prefabricated reinforced concrete floor slab[J]. IOP Conference Series Materials Science and Engineering, 2021, 1103(1):012023.
[10] Ra Gipani R, Escobar E, Prentice D, et al. Selective sulfur removal from semi-dry flue gas desulfurization coal fly ash for concrete and carbon dioxide capture applications[J]. Waste Management, 2021, 121(12):117–126.
[11] Tiberti S, Scuro C, Porzio S, et al. Post-Cracking B-FRCM Strengthening of a Traditional Anti-Seismic Construction Technique (Casa baraccata): Extensive Experimental Investigations[J]. Key Engineering Materials, 2019, 817(6):634–641.
[12] Ohsumi M, Nanazawa T, Tanimoto S, et al. Development of a Seismic-Performance Assessment Method and Retrofitting Technology Against

the Liquefaction of Existing Bridges[J]. Journal of Disaster Research, 2019, 14(2):269–278.

[13] Y Shi, Y Wang, Feng H, et al. Design, Fabrication and Test of a Low Range Capacitive Accelerometer With Anti-Overload Characteristics[J]. IEEE Access, 2020, 8(10):26085–26093.

[14] Luo Z, Xue J, Zhou T, et al. Shaking table tests and seismic design suggestions for innovative suspended ceiling systems with detachable metal panels[J]. Engineering Structures, 2021, 232(10):111830.

[15] Custodi A, Santopuoli N . Modeling and Design of the Restoration and Seismic Strengthening of the Sanctuary of Santa Maria Delle Grazie at Fornò under New Italian Rules NTC 2018[J]. Key Engineering Materials, 2019, 817(9):650–658.

[16] Moleiro F, Carrera E, Ferreira A, et al. Hygro-thermo-mechanical modelling and analysis of multilayered plates with embedded functionally graded material layers[J]. Composite Structures, 2020, 233(9):111442.

[17] Oliveira H L, Chateauneuf A, Leonel E D. Probabilistic mechanical modelling of concrete creep based on the boundary element method[J]. Advances in Structural Engineering, 2019, 22(2):337–348.

[18] Zhang J, Zhou J J, Cheng Z K, et al. Fabrication, Mechanical Modeling, and Experiments of a 3D-Motion Soft Actuator for Flexible Sensing[J]. IEEE Access, 2020, PP(99):1–1.

[19] Blanchard J M F A, Mutlu U, Sobey A J, et al. Modelling the different mechanical response and increased stresses exhibited by structures made from natural fibre composites[J]. Composite Structures, 2019, 215(MAY):402–410.

[20] Nonlinear modeling and characterization of ultrasoft silicone elastomers[J]. Applied Physics Letters, 2020, 116(20):203702.

[21] Musa S S, Zhao S, He D, et al. The Long-Term Periodic Patterns of Global Rabies Epidemics Among Animals: A Modeling Analysis[J]. International Journal of Bifurcation and Chaos, 2020, 30(3):2050047.

Biographies

Taochun Yang is a post-doctoral student at College of Civil Engineering and Architecture, Zhejiang University since 2018. He attended Tongji University, China where he received his M.Sc. degree and Ph.D. in structure Engineering in 2008 and 2014. Now he mainly engages in research work about FEA analysis and blast-resistance for structures.

Yanjun Li now works at the University of Jinan, China. He received his M.Sc. degree and Ph.D. in structure Engineering in 2007 and 2014 from Harbin Institute of Technology, China. He mainly engages in research work about FEA analysis and semi-resistance for structures.

Xiaohui Zhai now works at Ningbo Jiangong Engineering Group Co., Ltd. She studied at Ningbo University from 2015 to 2017. Her major is Civil Engineering. She has experiences in the simulation of structure as BIM engineer in Civil field.